Impact Of Hyperstoichiometry On The Solubility And Diffusion Rate Of Iodine In Fuel

M. Saidy[a], J.F. Mouris[b], W.H. Hocking[a] And R.A. Verrall[b]

[a]Reactor Chemistry and Corrosion Branch
[b]Fuel Development Branch
AECL, Chalk River Laboratories
Chalk River, Ontario, Canada, K0J 1J0

ABSTRACT

A novel out-reactor method has been developed over the past few years for investigating the migration behaviour of fission products in oxide nuclear fuels. This process allows the effects of thermal diffusion, radiation damage and local segregation to be independently assessed. Tailored fission-product concentration profiles are first created in the near-surface region of polished wafers by ion implantation. The impact of thermal annealing or simulated fission is then precisely determined by depth profiling with high-performance secondary ion mass spectrometry (SIMS). Thermal diffusion of iodine at a peak temperature of either 1200°C or 1400°C under slightly oxidizing conditions to achieve a nominal O/U ratio of either 2.01 or 2.02 was found to cause an increase in both the solubility and diffusion rate of iodine by two orders of magnitude compared to stoichiometric fuel. These effects are consistent with the increase in the number of uranium lattice vacancies predicted by a thermodynamic model for the defect structure of the uraninite lattice.

1. INTRODUCTION

The migration and segregation behaviour of fission products in oxide nuclear fuels are important factors for assessing performance and safety throughout the nuclear fuel cycle [1-4]. Release of inert fission gases from the fuel matrix can be sufficient, at high burnup, to cause overpressure strain of the fuel sheath. Several volatile fission products, notably iodine, have been implicated in fuel failures caused by stress-corrosion cracking of the Zircaloy sheath [5]. Release of radionuclides from defected fuel elements during reactor operation contributes to activity transport. Accumulation of segregated fission products at the fuel grain boundaries and at the fuel-sheath interface also enhances the potential for release of radioactivity to the environment throughout the nuclear fuel cycle [2-4]. Considerable effort has been expended over the past three decades to develop computer codes for predicting fuel performance, but there are still

large uncertainties in the experimental data used to calibrate the physical or empirical models.

Migration to the fuel grain boundaries is the first stage, and normally the rate-determining step, in segregation and release of volatile and noble-gas fission products [3]. Three distinct regimes have been recognized for the diffusion of fission products within the fuel matrix during reactor operation [6]. These are dependent upon whether the two processes necessary for diffusion—formation of vacancies and migration of vacancies—are predominantly controlled by thermal activation or radiation [6]. For temperatures below ~1000 K, migration has been shown to be athermal and directly proportional to the fission rate; this radiation-induced diffusion (RID) arises from transient thermal-spike and pressure-gradient effects that occur along fission tracks [7,8]. True thermal diffusion (TD), in which both the formation of lattice vacancies and the movement of fission products are thermally controlled, predominates only above ~1600 K [6,9]. At intermediate temperatures, fission products can move by thermally activated jumps between lattice vacancies created by radiation damage. This is termed radiation-enhanced diffusion (RED) [6,8]. Both TD and RED are strongly influenced by the stoichiometry of the fuel matrix [9-11], which directly affects the number of vacancies [12]. In particular, the concentration of uranium vacancies in UO_{2+x} increases rapidly as a function of x and provides an enhanced number of sites that can be occupied by migrating fission products [12]. Although modern nuclear fuel is almost exactly stoichiometric UO_2 (i.e. $x = 0$) prior to irradiation, excess oxygen can be present after extended burnup because the average valence of the combined fission products is slightly less than four [1]. Significant oxidation of the fuel in the event of either an individual sheath defect or a more serious accident can cause accelerated migration and release of fission products. If the solubility limit of a particular fission product in the fuel matrix is exceeded, precipitation as microscopic intragranular particles or bubbles can occur. These sites act as effective traps or sinks for that fission product, thereby inhibiting its migration through the fuel matrix, unless they are disrupted by fission spikes—radiation-induced dissolution [13,14].

Monitoring the release of radiotracers has been the standard method for assessing fission-product migration in nuclear fuels over the past four decades. However, the correct interpretation of such data can be very difficult and results spanning many orders of magnitude have been reported [6,9,10,15-19]. The Booth model has been widely used to analyse release data; it yields an effective diffusion coefficient, D/a^2, where a is the radius of a hypothetical sphere equivalent to the diffusion volume [20]. For experiments on polycrystalline ceramic fuels, evaluating the appropriate value of this sphere radius introduces considerable further uncertainty into the final result [15,18,21]. Direct measurement of the diffusive spreading of a concentrated source, such as a deposited film, which is generally recognized as the only reliable approach for determining diffusion coefficients, has historically been applied only to the lattice atoms of the oxide nuclear fuels [16,17,19,22]. An improved method for investigating the migration behaviour of fission products in UO_2 has been developed: changes in tailored fission-product distributions, which have been created in the near-surface region of polished wafers by ion implantation, as a result of annealing or simulated fission are

precisely determined by depth profiling with high-performance secondary ion mass spectrometry (SIMS) [23,24].

Buried layers of iodine, with near-Gaussian distributions, were created in polycrystalline UO_2 by ion-implantation to fluences spanning orders of magnitude. Diffusive spreading of iodine was induced by annealing under slightly oxidizing conditions to achieve a nominal O/U ratio of either 2.01 or 2.02. The partial differential equation that represents Fick's second law was numerically solved (using the *Mathematica* software package from Wolfram Research, Champaign, Illinois) to analyze diffusive spreading of the iodine and to determine accurate diffusion coefficients [25]. The effects of trapping at defect sites and excess vacancies caused by higher oxygen potential during annealing will be illustrated.

2. EXPERIMENTAL PROCEDURES

The experiments reported here were performed on polycrystalline UO_2 wafers ~2 mm thick, which had been sintered to ~97% of the theoretical density, with polygonal, equiaxed grains mainly 5-15 μm in size (fuel-grade ceramic). Mechanical damage created by polishing one face of each sample to a 0.05 μm finish was removed by annealing at 1500°C in an atmosphere of Ar-4%H_2 [26]. Tailored concentration profiles of I-127 were then introduced into the near-surface region of the polished face by ion implantation. Buried layers, with near-Gaussian distributions, at mean projected ranges between ~80 nm and ~165 nm, were created by employing ion-implantation energies in the 440 keV to 900 keV range. These layers were produced with a tandem accelerator operated by Interface Science Western at the University of Western Ontario (UWO). A focussed ion beam was rastered across the sample to ensure uniform implantation, and the wafers were later divided in two, three or four pieces to obtain identical duplicate samples. The implanted-ion fluence was either 10^{13} ions/cm^2 or 10^{15} ions/cm^2 for the present study, but measurements have also been made with 10^{11} ions/cm^2.

Diffusive spreading of the ion-implanted fission-product layer was induced by annealing at temperatures of either 1200°C or 1400°C in a high-density alumina tube furnace. The temperature was ramped up and down at a rate of 10°C/min, and was held at the maximum value for 150 min. Because of the exponential dependence of TD on temperature, lattice migration of iodine during the ramped portion of the anneal typically made only a minor contribution to the overall diffusive spreading. A type B thermocouple was used to monitor the in-situ temperature. Thermal annealing of the implanted samples was done under slightly oxidizing conditions to achieve a nominal O/U ratio of either 2.01 or 2.02.

A coulometric titration system was used to control the oxygen potential during anneals of the ion-implanted wafers [27]. The supply gas used was a mixture of 1300 ppm H_2 in argon. Prior to entering the furnace, the gas mixture was passed through a combination

electrolysis and measurement cell where a controlled amount of oxygen was added to the gas mixture. After being exposed to the sample at high temperature, the gas mixture passed through another electrolysis and measurement cell where the amount of oxygen absorbed by the ion-implanted sample was measured. In order to achieve a desired O/U ratio in the ion-implanted sample during the anneal process, standard UO_2 samples of a similar weight and shape to the ion implanted sample were tested to determine the oxygen potential required in the furnace [27].

The iodine distributions within both diffused and as-implanted samples were measured by secondary ion mass spectrometry with a Cameca IMS 6f SIMS instrument at Chalk River Laboratories (CRL). A double-focussing magnetic-sector mass spectrometer provides high throughput for secondary ions, which are detected with an electron multiplier operated in the single-ion counting mode. The pressure inside the sample chamber was $<10^{-9}$ Torr during the analyses. A Cs^+ primary-ion beam was used to enhance the yield of negative secondary ions when depth-profiling iodine (detected as I^-) [28]. A focussed 10 keV Cs^+ beam, with a diameter of ~30 μm and a current of 50 nA, was rastered over an area of 250 μm by 250 μm on the sample surface. Secondary ions were efficiently collected, using a 5 kV extraction field, from a smaller region (60 μm in size) located in the centre of the sputtered area to minimize crater-edge effects [28].

The depth scale for every profile was subsequently determined by measuring the depth of the sputtered crater using a Tencor Alpha-Step 500 stylus profilometer, which was routinely calibrated against a thin step-height standard (450±3 nm) from VLSI Standards Inc. Significant roughness developed in the bottom of the sputtered craters, arising from differences in sputtering rates for the various UO_2 grain orientations [23]. An average crater depth was then derived from eight line scans recorded across the central region of each crater in two different directions. Because about 100 grains are included in the analysis area, the effects of different grain orientations should be largely averaged out. Depth profiles were always recorded in pairs—one from a 'diffused' sample and the other from its as-implanted duplicate—under identical instrument operating conditions. In one case, both the reference and annealed samples were coated with a very thin film of gold before the SIMS analysis to confirm the absence of any artefacts associated with surface charging[1]. The concentration scale for the as-implanted sample was determined from the integrated area under the profile and the known implantation fluence [28]. A relative sensitivity factor (RSF) for I^- normalized to a matrix species could then be derived for these analytical conditions [28]. Finally, application of this RSF to the profile for the 'diffused' sample allowed its concentration scale to be calibrated—independent of any loss due to volatilization from the surface.

[1] Nearly stoichiometric uranium dioxide is a p-type semiconductor in which the majority charge carriers (holes) migrate by a small polaron hopping process [29]. Because the concentration of charge carriers is also a function of the stoichiometry, coating both reference and annealed wafers with a thin film of gold provides additional confidence that the results have not been influenced by surface charging effects.

Generally good agreement was obtained using U, UO and UO_2 as the matrix species for the RSF normalization.

Diffusion coefficients have been derived from the measured diffusive spreading of the implanted-ion distributions by numerically solving the partial differential equation that represents Fick's second law (using the *Mathematica* software package from Wolfram Research, Champaign, Illinois) [25].

3. RESULTS AND DISCUSSION

The impact of thermal annealing at 1400°C for 150 min under slightly oxidizing conditions (sufficient to produce $UO_{2.02}$) on the distribution of iodine ion-implanted into polycrystalline UO_2 at 440 keV to a fluence of 1×10^{13} ions/cm^2 is illustrated in Figure 1. Duplicate profiles recorded from the as-implanted as well as the annealed and oxidized samples demonstrate excellent reproducibility. Pronounced migration of iodine into the bulk matrix has clearly been achieved here over the entire implanted-ion distribution. Previous studies of stoichiometric UO_2 had revealed that iodine was trapped above concentrations of about 10^{16} atoms/cm^3 and migration was observed only in the tail of the distribution [24,30]. As illustrated in Figure 2, iodine remains trapped over the peak of the distribution at concentrations above 10^{16} atoms/cm^3 even after extended annealing at high temperatures under reducing conditions, although the peak concentration did decline due to loss from the surface as a result of radiation-enhanced diffusion associated with lattice vacancies created during the implantation process [23,24]. The maximum iodine concentration at the peak of the as-implanted reference profile in Figure 1 (about 9×10^{17} atoms/cm^3) is well above the threshold level (~10^{16} atoms/cm^3) identified for defect trapping [24,30]. Furthermore, a simple diffusion analysis, with a constant diffusion coefficient of 2×10^{-13} cm^2/s over the entire depth, provided a reasonable fit to the altered distribution, which is two orders of magnitude greater than the corresponding value (3×10^{-15} cm^2/s) determined for stoichiometric UO_2 at 1400°C [24,30,31].

A thermodynamic model of the defect structure of the fluorite lattice predicts equilibria between the various types of defects (oxygen interstitials, uranium lattice vacancies, etc.) [12]. The fraction of uranium lattice sites that are vacant in UO_{2+x} can then be directly related to the degree of hyperstoichiometry by the following expression:

$$V_U = x^2.\exp[-(\Delta G_S - 2\Delta G_{FO})/kT] \qquad (1)$$

where ΔG_S is the free energy of formation for a Schottky trio (a neutral trivacancy consisting of one uranium vacancy and two oxygen vacancies), ΔG_{FO} is the free energy of formation for an anti-Frenkel defect (an oxygen vacancy plus an oxygen interstitial), k is the Boltzmann constant and T is the absolute temperature. Thermodynamic data taken from the literature (ΔG_S = 6.2-6.4 eV and ΔG_{FO} = 3.0-3.1 eV) were used to

calculate V_U for the conditions of the experiment in Figure 2 (x = 0.02 and T = 1673 K) [32-34]. The absolute number density of uranium lattice vacancies, N_{VU}, could then be estimated (from $N_{VU} = V_U \cdot N_U$ where N_U is the number density of uranium atoms in UO_2) to be about 10^{18} vac/cm^3, which is just above the peak concentration of the as-implanted iodine distribution in Figure 1. A similar calculation for pure, stoichiometric UO_2 (without implanted iodine) yielded a much smaller concentration of uranium lattice vacancies at 1400°C ($N_{VU} \sim 10^{13}$ vac/cm^3) [12].

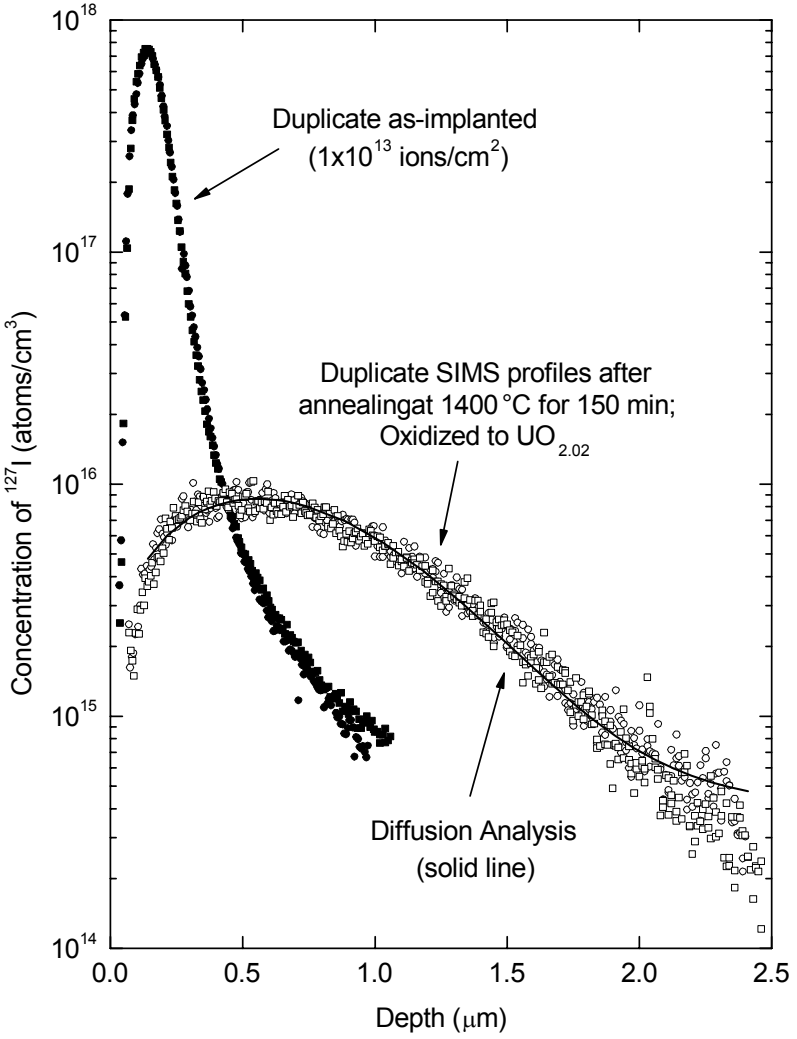

Figure 1. Depth Profiles of ^{127}I As-Implanted into Polycrystalline UO_2 at 440 keV to a Fluence of $1x10^{13}$ ions/cm^2 and After a 150 min Thermal Anneal at 1400°C Under Slightly Oxidizing Conditions to Produce $UO_{2.02}$.

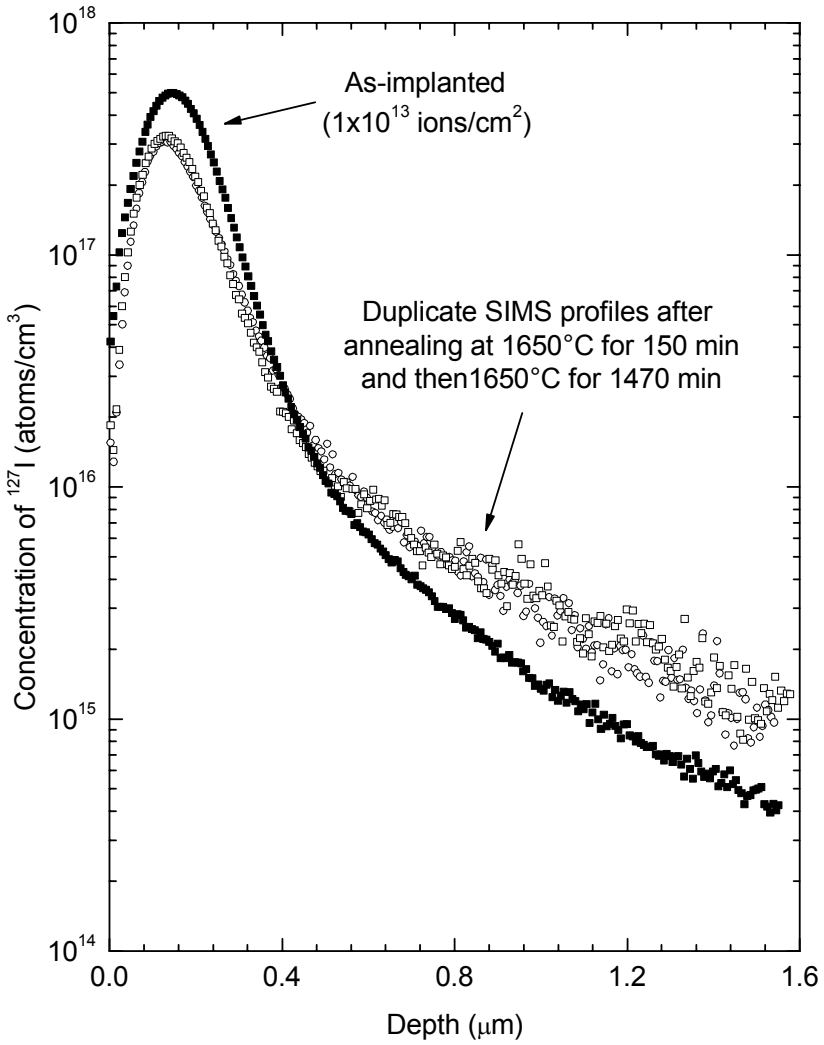

Figure 2. Depth Profiles of ^{127}I As-Implanted into Polycrystalline UO_2 at 900 keV to a Fluence of $1x10^{13}$ ions/cm^2 and After Thermal Anneling at 1650°C Under Reducing Conditions for Extended Periods.

The effects of thermal annealing at 1400°C for 150 min under slightly oxidizing conditions (sufficient to produce $UO_{2.02}$) on the depth distribution of iodine ion-implanted into polycrystalline UO_2 crystal at 440 keV to a fluence of 1×10^{15} ions/cm^2 are illustrated in Figure 3. Diffusive spreading of iodine is dramatically less pronounced here than was observed for the lower fluence case above (compare Figure 3 with Figure 1); instead, trapping effects clearly predominate over the peak of the distribution. The solubility limit for iodine in $UO_{2.02}$ has evidently been exceeded at concentrations above ~10^{18} atoms/cm^3, consistent with the estimated number density of uranium lattice vacancies under these conditions. Although there is some evidence of iodine migration on the backside of the profile, diffusive spreading in the tail of the distribution is surprisingly limited. The explanation for this behaviour is not apparent.

Thermal diffusion of iodine, ion-implanted into polycrystalline UO_2 at 440 keV to a fluence of 1×10^{13} ions/cm^2, at 1200°C for 150 min under slightly oxidizing conditions, sufficient to produce $UO_{2.01}$, is illustrated in Figure 4. Duplicate profiles recorded from the as-implanted as well as the annealed and oxidized wafer again show excellent reproducibility. Diffusive spreading of the iodine is less pronounced here than was observed after the 1400°C anneal of an equivalent sample oxidized to $UO_{2.02}$ (compare Figure 4 with Figure 1). Furthermore, there are some indications of trapping effects (the appearance of a flattened peak shifted towards the surface) right at the peak of the distribution, which suggests that the solubility limit was just exceeded at the maximum iodine concentration. This would be consistent with the fact that the number density of uranium lattice vacancies estimated using Equation (1) for the present conditions (1200°C and x = 0.01) is about a factor of five smaller than the value derived above (~10^{18} vac/cm^3 for 1400°C and x = 0.02). An approximate fit to the backside of the profile (with *Mathematica*) yielded a diffusion coefficient of 3.3×10^{-14} cm^2/s, which is two orders of magnitude greater than the corresponding value (3.5×10^{-16} cm^2/s) determined for stoichiometric UO_2 at 1200°C [31]. Furthermore, the mean diffusive spreading measured from the profiles in Figure 4 (0.15 μm) yields an estimated diffusion coefficient for iodine in $UO_{2.01}$ of 1.3×10^{-14} cm^2/s (from the $D = (\langle X \rangle)^2/(2.t)$ relationship derived by random-walk theory applied to the individual jumps over atomic distances, which has been found to provide a good estimate of diffusion coefficients [31,32]).

4. CONCLUSIONS AND FUTURE WORK

The combination of coulometric titration and ion-implantation/SIMS analyses has been shown to offer great potential for quantitatively determining the impact of hyperstoichiometry on iodine migration. Pronounced changes in iodine solubility as a function of the number of uranium lattice vacancies are clearly as important as enhanced thermal diffusion rates for influencing overall mobility and segregation tendency. Measurement of fission-product solubility at such low levels would be problematic using classical methods [1].

Because the diffusion rate of oxygen through the uraninite lattice is many orders of magnitude faster than that of fission products [12,16,17], the stoichiometry within the

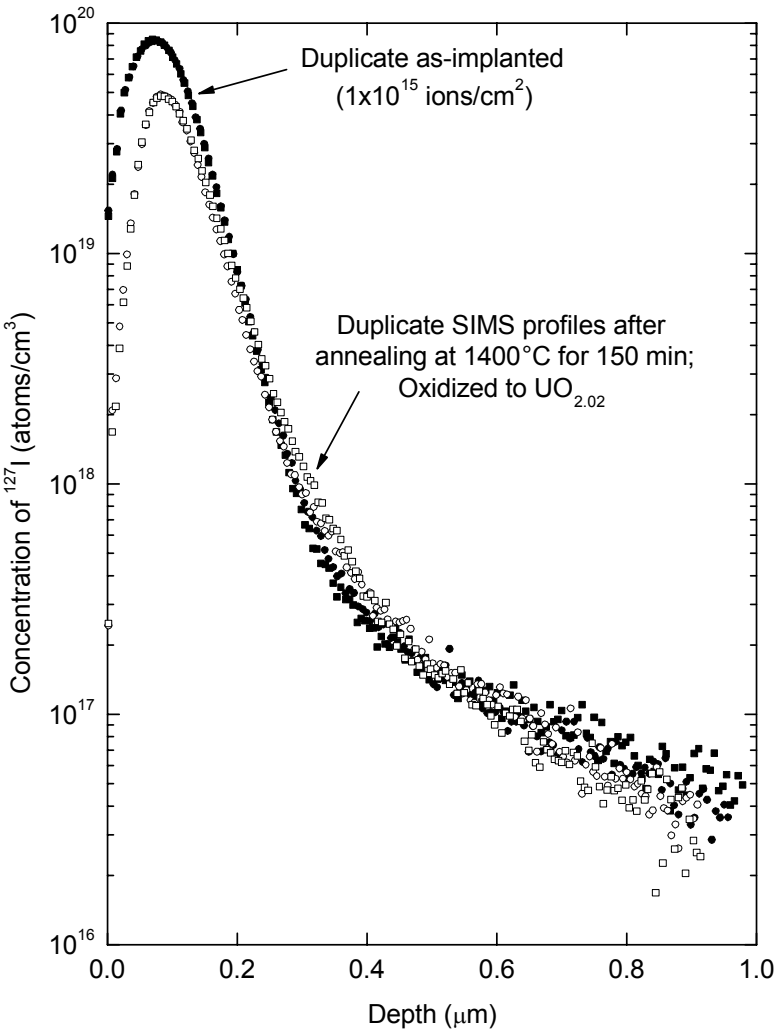

Figure 3. Depth Profiles of ^{127}I As-Implanted into Polycrystalline UO_2 at 440 keV to a Fluence of $1x10^{15}$ ions/cm^2 and After a 150 min Thermal Anneal at 1400°C Under Slightly Oxidizing Conditions to Produce $UO_{2.02}$.

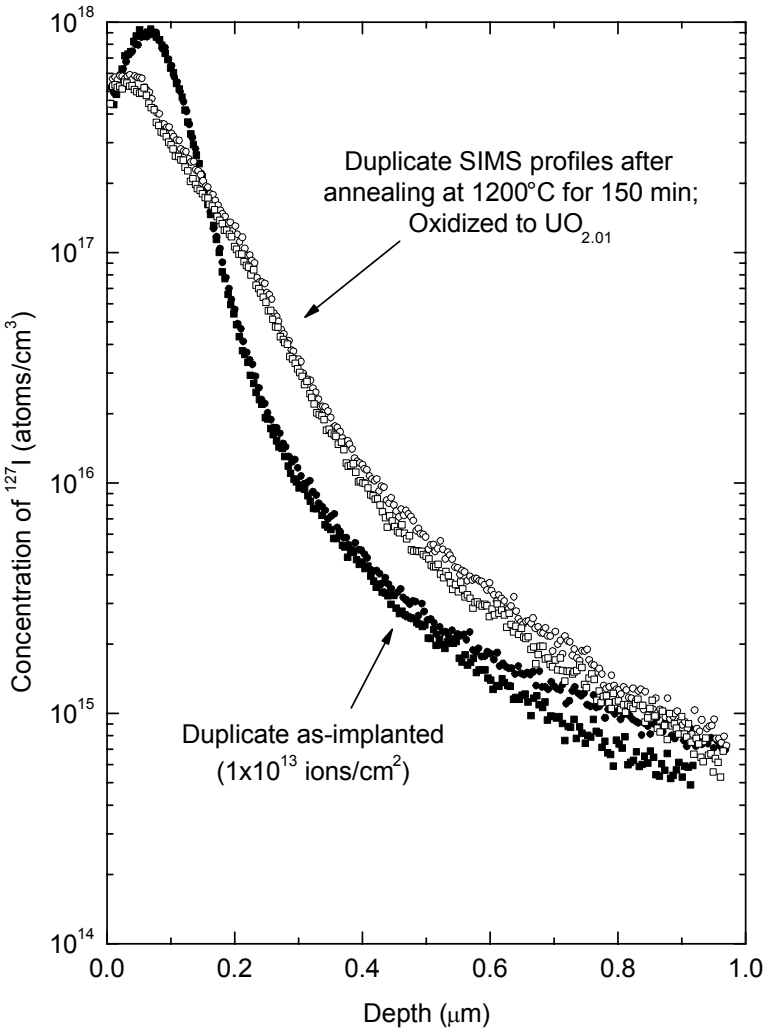

Figure 4. Depth Profiles of ^{127}I As-Implanted into Polycrystalline UO_2 at 440 keV to a Fluence of $1x10^{13}$ ions/cm^2 and After a 150 min Thermal Anneal at 1200°C Under Slightly Oxidizing Conditions to Produce $UO_{2.01}$.

shallow layer containing the implanted-ion distribution should remain uniform throughout the anneal at peak temperature. If the reaction kinetics at the surface are sufficiently slow [35], however, there could be some increase in the O/U ratio over the isothermal stage as well as during the initial upward ramp. Further evaluation of the oxidation process is warranted, which could lead to refinement of the coulometric titration strategy to optimize the experiment.

5. ACKNOWLEDGEMENTS

The authors would like to thank W.N. Lennard and J. Hendriks at the University of Western Ontario for performing the ion implantations.

6. REFERENCES

1. H. Kleykamp, “The Chemical State of the Fission Products in Oxide Nuclear Fuels”, Journal of Nuclear Materials, 131, 221-246 (1985).
2. J.R. Matthews, “Technological Problems and the Future of Research on the Basic Properties of Actinide Oxides”, Journal of the Chemical Society, Faraday Transactions 2, 83, 1271-1285 (1987).
3. J.H. Gittus, J.R. Matthews and P.E. Potter, “Safety Aspects of Fuel Behaviour During Faults and Accidents in Pressurized Water Reactors and in Liquid Sodium Cooled Fast-Breeder Reactors”, Journal of Nuclear Materials, 166, 132-159 (1989).
4. L.H. Johnson and D.W. Shoesmith, “Spent Fuel”, in “Radioactive Waste Forms for the Future”, Edited by W. Lutze and R.C. Ewing, Elsevier Science, Amsterdam, Chapter 11, 635-698 (1988).
5. B. Cox, “Pellet-Clad Interaction (PCI) Failures of Zirconium Alloy Fuel Cladding—A Review”, Journal of Nuclear Materials, 172, 249-292 (1990).
6. J.A. Turnbull, C.A. Friskney, J.R. Findlay, F.A. Johnson and A.J. Walter, “The Diffusion Coefficients of Gaseous and Volatile Species During the Irradiation of Uranium Dioxide”, Journal of Nuclear Materials, 107, 168–184 (1982).
7. Hj. Matzke, “Radiation Damage in Crystalline Insulators, Oxides and Ceramic Nuclear Fuels”, Radiation Effects, 64, 3–33 (1982).
8. H.Wollenberger, V. Naudorf and M.P. Macht, “Radiation-Induced Diffusion in Nuclear Materials”, in “Diffusion Processes”, Edited by R.P. Agarwala, Elsevier, Amsterdam 201-234 (1992).
9. M. Hirai, J.H. Davies and R. Williamson, “Diffusivities of Fission Gas Species in UO_2 and $(U,Gd)O_2$ Nuclear Fuels During Irradiation”, Journal of Nuclear Materials, 226, 238–251 (1995).
10. R.Lindner and Hj. Matzke, “The Diffusion of Xenon-133 in Uranium Oxide of Varying Oxygen Content”, Zeitschrift fur Naturforschung, 14a, 582–584 (1959).
11. J.C. Killen and J.A. Turnbull, “An Experimental and Theoretical Treatment of the Release of ^{85}Kr from Hyperstoichiometric Uranium Oxide”, Proceedings of a

Workshop on Chemical Reactivity of Oxide Fuel and Fission Product Release, Volume 2, Edited by K.A. Simpson and P. Wood, Berkeley Nuclear Laboratories, UK, 387-404 (1987).
12. Hj. Matzke, "Diffusion in Ceramic Oxide Systems", Advances in Ceramics, 17, 1-54 (1986).
13. J.A. Turnbull and R.M. Cornell, "The Re-Solution of Fission-Gas Atoms from Bubbles During the Irradiation of UO_2 at an Elevated Temperature", Journal of Nuclear Materials, 41, 156–160 (1971).
14. H. Blank and Hj. Matzke, "The Effect of Fission Spikes on Fission Gas Re-Solution", Radiation Effects, 17, 57–64 (1973).
15. Hj. Matzke, "Gas Release Mechanisms in UO_2—A Critical Review", Radiation Effects, 53, 219–242 (1980).
16. Hj. Matzke, "Atomic Transport Properties in UO_2 and Mixed Oxides $(U,Pu)O_2$", Journal of the Chemical Society, Faraday Transactions 2, 83, 1121–1142 (1987).
17. Hj. Matzke, "Diffusion Processes in Nuclear Fuels", in "Diffusion Processes", Edited by R.P. Agarwala, Elsevier, Amsterdam, 9-69 (1992).
18. M.A. Mansouri and D.R. Olander, "Fission Product Release from Trace Irradiated UO_{2+x}", Journal of Nuclear Materials, 254, 22–33 (1998).
19. W.H. Hocking, R.A. Verrall, P.G. Lucuta and Hj. Matzke, "Depth-Profiling Studies of Ion-Implanted Cesium and Rubidium in SIMFUEL and Uranium Dioxide", Radiation Effects and Defects in Solids, 125, 299–321 (1995).
20. A.H. Booth, "A Method of Calculating Fission Gas Diffusion from UO_2 Fuel and its Application to the X-2-f Loop Test", Atomic Energy of Canada Limited Report, CRDC-721 and AECL-496 (1957).
21. S.G. Prussin, D.R. Olander, W.K. Lau and L. Hansson, "Release of Fission Products (Xe, I, Te, Cs, Mo and Tc) from Polycrystalline UO_2", Journal of Nuclear Materials, 154, 25–37 (1988).
22. A.C.S. Sabioni, W.B. Ferraz and F. Millot, "First Study of Uranium Self-Diffusion in UO_2 by SIMS", Journal of Nuclear Materials, 257, 180–184 (1998).
23. W.H. Hocking, R.A. Verrall and S.J. Bushby, "A New Technique to Measure Fission-Product Diffusion Coefficients in UO_2 Fuel", International Atomic Energy Agency Technical Committee Meeting Proceedings, IAEA-TECDOC-1122, 111–118 (1999).
24. W.H. Hocking, R.A. Verrall and I.J. Muir, "Migration Behaviour of Iodine in Nuclear Fuel", Journal of Nuclear Materials, 294, 45–52 (2001).
25. H.S. Carlslaw and J.C. Jaeger, "Conduction of Heat in Solids", Second Edition, Clarendon, Oxford (1959).
26. Hj. Matzke and A. Turos, "Surface Damage in UO_2 Due to Mechanical Polishing and Ion Bombardment", Journal of Nuclear Materials, 114, 349–352 (1983).
27. R.A. Verrall, J.F. Mouris and Z. He, "O/M Ratio Measurement Techniques", Proceedings of the 8th International Conference on CANDU Fuel, Edited by D.B. Sanderson, Canadian Nuclear Society, Honey Harbour, Ontario, 65-73 (2003).
28. R.G. Wilson, F.A. Stevie and C.W. Magee, "Secondary Ion Mass Spectrometry: A Practical Handbook for Depth Profiling", Wiley, New York (1989).

29. D.W. Shoesmith, S. Sunder and W.H. Hocking, "Electrochemistry of UO_2 Nuclear Fuel", Chapter 6 in "Electrochemistry of Novel Materials", Edited by J. Lipkowski and P.N. Ross, VCH, New York, 297-337 (1994).
30. M. Saidy, R.A. Verrall, J.F. Mouris, I.J. Muir and W.H. Hocking, "Migration Behaviour of Fission Products in CANDU Fuel", Proceedings of the 8th International Conference on CANDU Fuel, Edited by D.B. Sanderson, Canadian Nuclear Society, Honey Harbour, Ontario, 137-148 (2003).
31. M. Saidy, W.H. Hocking, G. Carlot, P. Garcia and B. Pasquet, "International Collaboration on Assessing the Migration Behaviour of Iodine and Xenon in Oxide Nuclear Fuels", Atomic Energy of Canada Limited Report, 153-124600-440-001 (2005).
32. Hj. Matzke, "Diffusion in Nonstoichiometric Oxides", Chapter 4 in "Nonstoichiometric Oxides", Edited by O.T. Sorensen, Academic Press, New York, 155-232 (1981).
33. Hj. Matzke, "On Uranium Self-Diffusion in UO_2 and UO_{2+x}", Journal of Nuclear Materials, 30, 26-35 (1969).
34. Hj. Matzke, "Lattice Defects and Irradiation Damage in ThO_2, UO_2 and $(U,Pu)O_2$", Proceedings of the 5th International Conference on Plutonium and Other actinides, Edited by H. Blank and R. Lindner, North-Holland, Amsterdam, 801-831 (1976).
35. J. Abrefah, A. de Aguiar Braid, W. Wang, Y. Khalil and D.R. Olander, "High Temperature Oxidation of UO_2 in Steam-Hydrogen Mixtures", Journal of Nuclear Materials, 208, 98-110 (1994).